

# High quality ZrC, ZrC/ZrN and ZrC/TiN thin films grown by pulsed laser deposition

D. CRACIUN<sup>a</sup>, G. SOCOL<sup>a</sup>, G. DORCIOMAN<sup>a</sup>, N. STEFAN<sup>a</sup>, G. BOURNE<sup>b</sup>, V. CRACIUN<sup>a,b,\*</sup>

<sup>a</sup>Laser Department, National Institute for Laser, Plasma, and Radiation Physics, Bucharest, Romania

<sup>b</sup>Major Analytical Instrumentation Center, Materials Science and Engineering, University of Florida, Gainesville, FL 32611, USA

ZrC, ZrC/ZrN, and ZrC/ZrTiN films were grown on (100) Si substrates by the pulsed laser deposition (PLD) technique using a KrF excimer laser working at 40 Hz and 8 J/cm<sup>2</sup>. The nominal substrate temperature during depositions was 300 °C and the cooling rate was 5 °C/min. X-ray diffraction investigations showed that films were crystalline, the grain size depending on the nature and pressure of the gas used during deposition. The films elemental composition, analyzed by Auger electron spectroscopy (AES) and x-ray photoelectron spectroscopy (XPS), showed the presence of a carboxide layer in the surface region. After its removal by Ar ion sputtering, the oxygen concentration rapidly decreased, down to around 4-6 % in bulk. Simulations of the x-ray reflectivity (XRR) curves indicated a smooth surface morphology, with roughness below 1 nm (rms) and films density around 95-97 % of bulk values. While nanoindentation results showed for the best quality ZrC films a hardness of 27.6 GPa and a reduced modulus of 228 GPa, multilayer ZrC/ZrN and ZrC/ZrTiN samples exhibited hardness and reduced modulus values between 32.4 to 33.2 GPa and 251-270 GPa, respectively.

(Received June 19, 2009; accepted October 12, 2009)

**Keywords:** Laser ablation, ZrC, ZrN, TiN, Nanoindentation

## 1. Introduction

New and important applications of ZrC such as nuclear fuel particles coatings, field emitter coatings, or thermophotovoltaic radiator coatings [1-4] have driven the interest for obtaining high quality thin films. Progress has been made in obtaining good quality ZrC films that exhibited hardness values from 20 to 27 GPa and reduced Young modulus of 200-300 GPa by using either physical vapor deposition (PVD) or chemical vapor deposition (CVD) based techniques [5-11]. The pulsed laser deposition (PLD) technique has been successfully employed to deposit ZrC films [12-17]. Such films exhibited very good mechanical properties, with hardness values up to 31.0 GPa, low oxygen contamination and good crystalline quality. We investigated ways to further improve the quality of ZrC films deposited by PLD by optimizing the processing parameters or by depositing multilayers of ZrC and a refractory metal nitride such as ZrN or TiN.

## 2. Experiment

The depositions were performed in a PLD system using a KrF excimer laser ( $\lambda=248$  nm, pulse duration  $\tau = 25$  ns, 8.0 J/cm<sup>2</sup> fluence, 40 Hz repetition rate). Some films were deposited using a rectangular aperture of 1x2 cm<sup>2</sup>, located adjacent to the laser exit mirror, that selected only the central and more uniform part of the laser beam, maintaining the same fluence. To ensure adequate thickness for nanoindentation measurements, films were

deposited for tens of minutes from polycrystalline ZrC, ZrN, and TiN targets (Plasmaterials, Inc.) on p<sup>++</sup> (100)Si substrates supplied by MEMC Electronic Materials, Inc. Prior to being loaded into the deposition chamber, the substrates were cleaned in acetone, then ethanol, rinsed in deionized water, and finally blown dry with high purity nitrogen. The nominal substrate temperature was set at 300 °C. Depositions were performed under a high purity CH<sub>4</sub> or Ar atmosphere ( $2 \times 10^{-3} - 2 \times 10^{-2}$  Pa). After deposition, films were cooled down to room temperature at a rate of approximately 5 °C / min under the same atmosphere as that used during deposition but at a much higher pressure.

The films mass density, thickness, and surface and interfacial roughness were investigated by x-ray reflectometry (XRR, Panalytical X'Pert MRD system, using Cu K <sub>$\alpha$</sub>  radiation). The same instrument was used for structural characterization in symmetric and grazing incidence x-ray diffraction (XRD and GIXD). The chemical composition of the films was investigated by Auger electron spectroscopy (AES) in a Perkin-Elmer PHI 660 system and by x-ray photoelectron spectroscopy (XPS) in a Perkin-Elmer PHI 5100 ESCA system. To obtain elemental depth profiles, measurements were collected after various time cycles of Ar ion sputtering (4 kV, 1-3  $\mu$ A/cm<sup>2</sup>; for XPS measurements the Ar ion beam was rastered over a 10 x 7 mm<sup>2</sup> area).

The mechanical properties of the films were measured with a nanoindentation device (Hysitron inc.) equipped with a cube-corner diamond tip and set to run 100 or 300 indents per sample. The indentation experiments were performed in displacement control with a contact depth of

up to 35 nm to exclude substrate contributions. The tip geometry was characterized by indentation in a standard fused quartz sample and an area vs. displacement function was curve fit from the data [18]. Hardness and reduced modulus were determined from the load-displacement data following the model of Oliver and Pharr [18].

### 3. Results and discussion

XRD and GIXD investigations showed that the deposited films were crystalline, as one can see in Fig. 1, where diffraction patterns acquired in symmetrical incidence geometry (theta-2theta) are displayed. One can note that the use of the aperture (mentioned as “mask” in Fig. 1) did not improve the crystallinity of the ZrC films as compared to the highest crystallinity films obtained under  $2 \times 10^{-3}$  Pa  $\text{CH}_4$ . However, it is worth mentioning that the films deposited using the aperture exhibited small shifts in the diffraction line positions towards those observed for the ZrC target or the powder standard, an indication of stress relaxation. Also, the films maintained the (002) texture, although it was weaker than that observed for films deposited under optimized conditions. Nanoindentation results, displayed in Table 1, together with the deposition conditions, showed that the films deposited using the aperture under  $2 \times 10^{-2}$  Pa and  $2 \times 10^{-3}$  Pa of  $\text{CH}_4$  exhibited hardness values of 24.7 to 25.7 GPa and 26.0 to 26.5 GPa, respectively. Such values are an improvement for films deposited at the higher  $\text{CH}_4$  pressure but not for the lower  $\text{CH}_4$  pressure. In addition, according to the XRR curve simulations, the films surface was smoother, interfaces were more abrupt, and their density marginally higher, from 6.4 to 6.5  $\text{g}/\text{cm}^3$ . These results indicated that the amount of ZrC material ablated during the action of a single pulse is important for achieving a high crystalline quality film, a conclusion also reached from the study of the role of laser fluence [14-15].

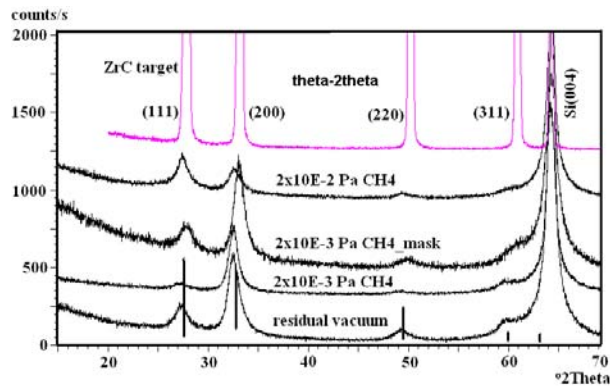


Fig. 1. XRD patterns collected from the ZrC target and deposited films; the vertical lines are the reference diffraction peak positions of ZrC powder [19].

Table 1. Deposition parameters and mechanical properties of grown films.

Sample	Deposition atmosphere	Number of pulses and multilayers	Hardness (GPa)	Reduced Modulus (GPa)
ZrC_1	$2 \times 10^{-3}$ Pa of $\text{CH}_4$	48000	27.1-27.9	225-228
ZrC_2D	$2 \times 10^{-2}$ Pa of $\text{CH}_4$	48000	24.7-25.7	187-189
ZrC_3D	$2 \times 10^{-3}$ Pa of $\text{CH}_4$	48000	26.0-26.5	204-229
ZrC-ZrN_1	$3 \times 10^{-3}$ Pa of $\text{CH}_4$	(750+750)x20	24.7-28.5	219-236
ZrC-ZrN_2	$3 \times 10^{-3}$ Pa of $\text{CH}_4$	(750+750)x20	29.8-32.4	236-252
ZrC-TiN_1	$10^{-2}$ Pa of Ar	(1500+1500)x20	27.0-28.2	225-230
ZrC-TiN_2	$5 \times 10^{-3}$ Pa of Ar	(1500+1500)x20	32.5-33.2	264-270

Carbides are usually harder but more brittle than nitrides and to further improve the mechanical properties we deposited samples consisting of multilayers of ZrC and either ZrN or TiN. Fig. 2 presents the XRD and GIXD patterns acquired on three locations (5 mm apart) of a film consisting of 20 layers of ZrC and 20 of ZrN. It is apparent that the ZrN diffraction peaks are absent, only those corresponding to ZrC being present. One can note that the texture of the film changed to (111). However, the hardness values measured in two locations were even better than those measured for ZrC films (see Fig. 3), suggesting that either the texture is not important [15, 16] or the multilayer structure results in a hardness increase [11, 20, 21, 22]. Despite the fact that atoms or ions inside a laser plasma present a laterally variation of the kinetic energies [23], the film crystallinity measured in three different locations was identical but the hardness was quite different. These results suggest that the thickness of each deposited layer in the multilayer structure is important. XRR curves displayed in Fig. 4 showed that there are changes in the layer thickness across the sample surface, as expected for PLD grown films. Since the thickness of the layers in the stack should be optimized to achieve the maximum hardness value [11, 20-22], it might be very advantageous to deposit such multilayer samples by PLD to study the effect of the layer thickness on the mechanical properties, rather similar to the well known combinatorial technique: the resulting multilayer film will exhibit a variable thickness laterally, making the optimization process faster [24].

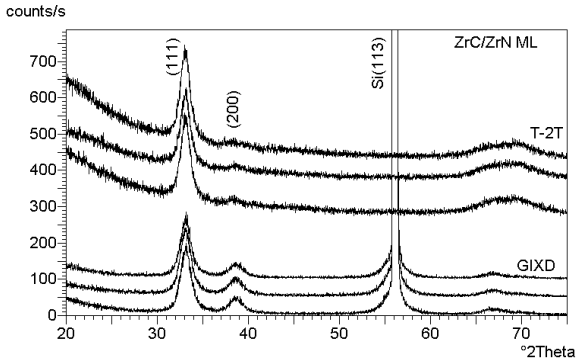


Fig. 2. Symmetrical XRD (upper traces) and GIXD (lower traces) patterns collected from three different locations on the ZrC-ZrN\_1 multilayer sample.

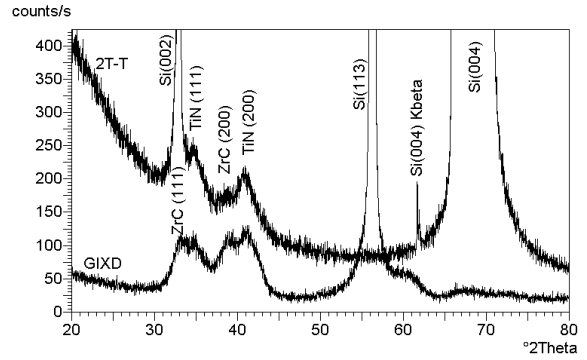


Fig. 5. Symmetrical XRD (upper trace) and GIXD (lower trace) patterns collected from the ZrC-TiN\_1 multilayer sample.

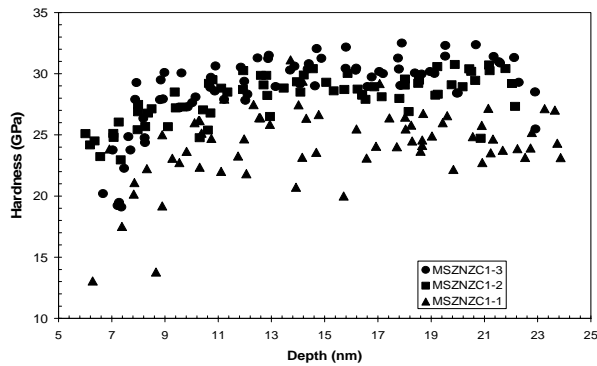


Fig. 3. Hardness versus contact depth results for the same three locations on the ZrC-ZrN\_1 multilayer sample.

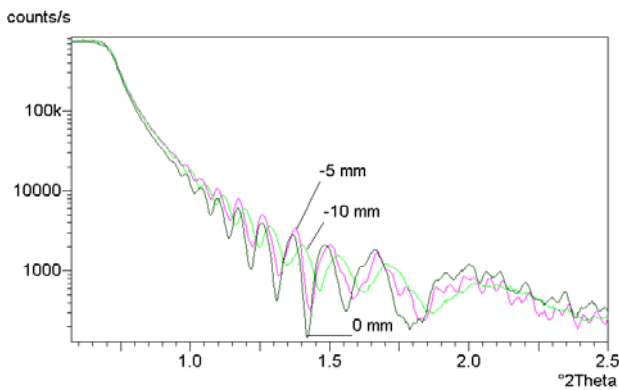


Fig. 4. XRR curves recorded for the same three locations on the ZrC-ZrN\_1 multilayer sample.

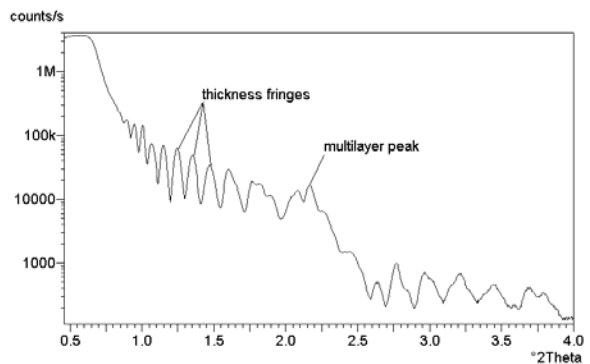


Fig. 6. XRR curve recorded for the ZrC-TiN\_1 multilayer sample.

Fig. 5 displays the XRD and GIXD patterns collected from the ZrC-TiN<sub>1</sub> multilayer sample. Both the ZrC and the TiN diffraction peaks are presented. The films are not very well crystallized and there is almost no texture. The XRR curve recorded from the same sample is shown in Fig. 6. The Kiessig fringes [25] are better resolved than for the ZrC/ZrN sample. The density of the layers, obtained from simulations of the XRR curves with the WinGixa software program from Panalytical indicated values around 6.4-6.5 g/cm<sup>3</sup> for the ZrC layers and 5.2-5.3 g/cm<sup>3</sup> for the TiN layers. A superlattice peak due to the layers presence is also visible. The nanohardness values measured for this sample were better than those measured for the ZrC/ZrN sample, probably because there was no so much intermixing, the interfaces being sharper and the TiN layers better crystallized.

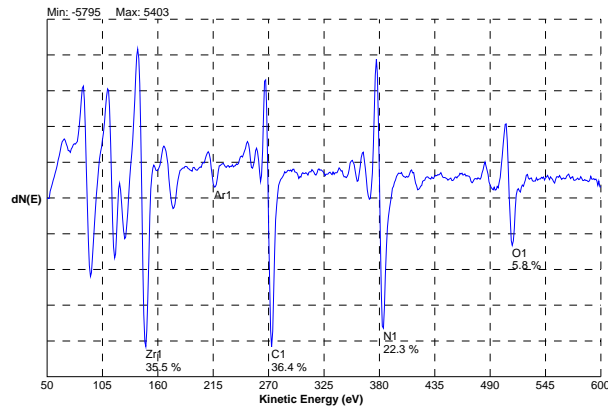


Fig. 7. AES spectrum acquired from the bulk region (after 5 min sputtering) of the ZrC-ZrN<sub>1</sub> multilayer sample.

Fig. 7 displays the AES spectrum corresponding to the bulk region of the ZrC-ZrN<sub>1</sub> multilayer sample. An oxygen concentration of 5.8% was measured, a little bit higher than the best value of 3.0% recorded for the optimized ZrC film. It appears that some oxidation occurred during deposition because of the longer time required to grow the 20 multilayer structure as compared with the deposition of a pure ZrC film. An elemental depth profile for the same sample is shown in Fig. 8. One can note that oscillations of the C and N signals are visible only for the first 3 deposited layers; after that, the composition variations are no longer visible, the sample exhibiting a mixed composition, as also suggested by the XRR and XRD results.

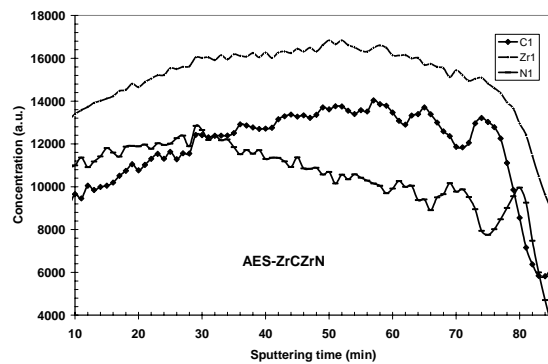


Fig. 8. AES depth profile acquired from the ZrC-ZrN<sub>1</sub> multilayer sample.

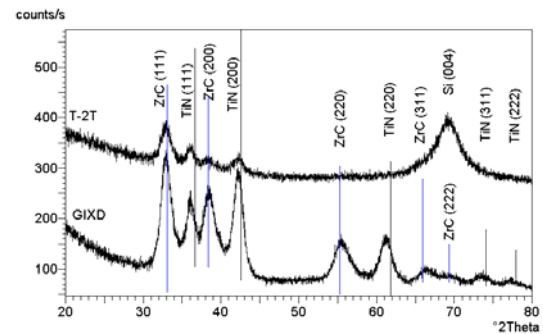


Fig. 9. Symmetrical XRD (upper trace) and GIXD (lower trace) patterns collected from the ZrC-TiN<sub>2</sub> multilayer sample; the vertical bars indicate the standard position of ZrC and TiN compounds.

Based on these results we deposited samples containing thicker layers. Fig. 9 presents the XRD and GIXD patterns acquired from the ZrC-TiN<sub>2</sub> multilayer sample. The vertical lines correspond to standard ZrC and TiN powders. One can note the improved crystallinity of this sample as compared to the one with thinner layers. The nanoindentation results, presented on Table 1 showed significantly better values than those measured for the best ZrC sample, both for hardness and reduced modulus.

#### 4. Conclusions

The structure and mechanical properties of ZrC and ZrC/ZrN and ZrC/TiN multilayer structures were investigated. ZrC thin films deposited using an aperture that selected the central, more uniform part of the laser beam showed marginal improvements in surface morphology, density and stress. However, they were not harder than films deposited without this aperture. A significant improvement of the hardness and reduced modulus were obtained by depositing ZrC/ZrN and ZrC/TiN multilayer structures. By optimizing the thickness of layers in the multilayer structure a nanoindentation value of 33.2 GPa was measured for a ZrC/TiN sample.

#### Acknowledgements

We would like to acknowledge the Major Analytical Instrumentation Center for help with samples characterization. This work was partially funded by CNCSIS Ideas Project code 1408.

## References

- [1] C. M. Hollabaugh, L. A. Wahman, R. D. Reiswig, R.W. White, P. Wagner, Nucl. Technol. **35**, 527 (1997).
- [2] F. M. Charbonnier, W. A. Mackie, R. L. Hartman, T. Xie, J. Vac. Sci. Technol. **B19**, 1064 (2001).
- [3] T. Xie, W.A. Mackie, P.R. Davis, J. Vac. Sci. Technol. **B14**, 2090 (1996).
- [4] R. Ganter, R. Bakker, C. Gough, S. C. Leemann, M. Paraliiev, M. Pedrozzi, F. Le Pimpec, V. Schlott, L. Rivkin, A. Wrulich, Phys. Rev. Lett. **100**, 064801 (2008).
- [5] J. A. Glass, N. Palmasio, R.E. Welsh, in: Properties and Processing of Vapor-Deposited Coatings, M. Pickering, B.W. Sheldon, W.Y. Lee, R.N. Johnson (Eds), Materials Research Society Symposium Proceeding **555**, 185 (1999).
- [6] B. V. Cockeram, J. L. Hollenbeck, Surf. Coat. Technol. **157**, 274 (2002).
- [7] Y. S. Won, Y. S. Kim, V. G. Varanasi, O. Kryliouk, T. J. Anderson, C. T. Sirimanne, L. McElwee-White, J. Cryst. Growth **304**, 324 (2007).
- [8] H. Li, M. Ding, J. Feng, X. Li, G. Bai, F. Zhang, J. Vac. Sci. Technol. **B24**, 1436 (2006).
- [9] J. E. Krzanowski, J. Wormwood, Surf. Coat. Technol. **201**, 2942 (2006).
- [10] M. Braic, V. Braic, M. Balaceanu, G. Pavelescu, A. Vladescu, J. Optoelectron. Adv. Mater. **5**(5), 1399 (2003).
- [11] M. Braic, M. Balaceanu, A. Vladescu, A. Kiss, V. Braic, A. Purice, G. Dinescu, N. Scarisoreanu, F. Stokker-Cheregi, A. Moldovan, R. Birjega M. Dinescu, Surface and Coatings Technology, **200**( 22-23) 6505 (2006).
- [12] L. D'Alessio, A. Santagata, R. Teghil, M. Zaccagnino, I. Zaccardo, V. Marotta, D. Ferro, G. De Maria, Appl. Surf. Sci. **168**, 284 (2000).
- [13] D. Ferro, J.V. Rau, V. Rossi Albertini, A. Generosi, R. Teghil, S.M. Barinov. Surface and Coatings Technology **202**, 1455 (2008).
- [14] V. Craciun, J. Woo, D. Craciun, R. K. Singh, Appl. Surf. Sci. **252**, 4615 (2006).
- [15] J. Woo, G. Bourne, V. Craciun, D. Craciun, R. K. Singh, J. Optoelectron. Adv. Mater. **8**, 20 (2006).
- [16] V. Craciun, D. Craciun, J. M. Howard, J. Woo, Thin Solid Films, **515**, 4636 (2007).
- [17] D. Craciun, G. Socol, N. Stefan, G. Bourne, V. Craciun, Appl. Surf. Sci., **255**, 5260 (2009).
- [18] W. C. Oliver, G. M. Pharr, J. Mater. Res., **47**, 1564 (1992).
- [19] JCPDS-International Center for Diffraction Data Copyright © JCPDS-ICDD 1996, card 35-0784 and card 32-1489.
- [20] G. Abadias, S Dub, R Shmegeera, Surface & Coatings Technology, **200**, 6538 (2006).
- [21] Li D. J., Yang J, Zhang X. H., Cao M., J. Vac. Technol. B, **25**, L11 (2007).
- [22] Yu L. H., Dong S. R., Xu J. H., Kojima I., Thin Solid Films **516**, 1864 (2008).
- [23] D. O'Mahony, J. Lunney, T. Dumont, S. Canulescu, T. Lippert, A. Wokaunb, Appl. Surf. Sci., **254**, 811 (2007).
- [24] N. D. Bassim, P. K. Schenck, M. Otani, H. Oguchi Rev. Sci. Instrum, **78**, 072203 (2007).
- [25] H. Kiessig, Ann. Phys., **10**, 769 (1931).

\*Corresponding author: vcrac@mse.ufl.edu